Kondo temperature and screening extension in a double dot system.

L. C. Ribeiro,[1] E. Vernek,[2] G. B. Martins,[3,*] and E. V. Anda[4]

[1]*Centro Federal de Educação Tecnológica Celso Suckow da Fonseca (CEFET-RJ/UnED-NI), RJ, 26041-271, Brazil*
[2]*Instituto de Física, Universidade Federal de Uberlândia, Uberlândia 38400-902, MG, Brazil*
[3]*Department of Physics, Oakland University, Rochester, Michigan 48309, USA*
[4]*Departamento de Física, Pontifícia Universidade Católica do Rio de Janeiro, 22453-900, Brazil*

In this work we use the Slave Boson Mean Field Approximation at finite U to study the effects of spin-spin correlations in the transport properties of two quantum dots coupled in series to metallic leads. Different quantum regimes of this system are studied in a wide range of parameter space. The main aspects related to the interplay between the half-filling Kondo effect and the antiferromagnetic correlation between the quantum dots are reviewed. Slave boson results for conductance, local density of states in the quantum dots, and the renormalized energy parameters, are presented. As a different approach to the Kondo physics in a double dot system, the Kondo cloud extension inside the metallic leads is calculated and its dependence with the inter-dot coupling is analyzed. In addition, the cloud extension permits the calculation of the Kondo temperature of the double quantum dot. This result is very similar to the corresponding critical temperature T_c, as a function of the parameters of the system, as obtained by using the finite temperature extension of the Slave Boson Mean Field Approximation.

PACS numbers: 73.23.Hk, 72.15.Qm, 73.63.Kv

I. INTRODUCTION

The Kondo regime in strongly correlated mesoscopic structures has been extensively studied since its observation in a single quantum dot (QD) connected to metallic leads.[1] The increasing interest in investigating the underlying physics of these structures is motivated by potential technological applications, such as the design of single electron transistor devices based on the Coulomb blockade effect, as observed in single QDs.[2,3] A system composed of two tunnel coupled QDs connected in series with metallic leads [henceforth called a double QD (DQD)] is particularly interesting because it is the simplest geometry in which the interplay of two energy scales determines its physical properties: (*i*) the Kondo correlation between the spin of each QD and the spins of the conduction electrons, and *(ii)* the antiferromagnetic correlation between the spins of the two QDs. Each of these two regimes prevail in different regions of the parameter space and compete in the crossover region. As discussed below, these regimes are manifested very clearly in charge transport measurements.

Several experimental and theoretical works have appeared in the last decade studying DQDs. The continued interest in DQDs stems from the early recognition[4,5] of a possible Non Fermi Liquid (NFL) Quantum Critical Point (QCP) separating a Fermi Liquid (FL) local singlet antiferromagnetic-phase from a Kondo screened FL Kondo-phase in the Two Impurity Kondo model (TIKM).[6] Subsequent Numerical Renormalization group (NRG)[7] calculations on the Two Impurity Anderson model (TIAM) detailed the properties of this NFL QCP,[8] but already pointed out that the inter-impurity hopping suppresses the critical transition.[9] The great flexibility of mesoscopic systems, especially semiconducting lateral QDs, where a continuous tuning of the relevant physical parameters is possible, lead to a series of detailed theoretical studies of DQDs as a prototype for the TIAM and TIKM. Several papers used different flavors of the Slave Boson formalism to analyze either the TIAM[10–15] and the TIKM.[16,17] Detailed studies have also been done using NRG,[8,18] the Embedded Cluster Approximation (ECA),[19] and the Non-Crossing Approximation.[20] The results obtained confirmed that when the even-odd parity symmetry is broken, the critical transition is replaced by a crossover. In addition, in the TIAM, it was found that, as the inter-dot hopping increases, a coherent superposition of the many-body Kondo states of each QD (forming bonding and antibonding combinations) results in a splitting of the Kondo resonance, which leads to a splitting of the zero bias anomaly in the differential conductance.[11,12,19] These many-body molecular states should not be confused with the single-particle molecular states (separated by an energy equal to twice the inter-dot hopping). In reality, the coherent single-particle molecular states were the first to be observed by R. H. Blick *et al.*[21] through careful analysis of the charging diagram of a DQD. Concurrently, by using a combination of charge transport and microwave spectroscopy, Oosterkamp *et al.*[22] probed the formation of single-particle molecular states (which they called 'covalent bonds') in a DQD by varying the tunneling coupling between the QDs, showing the possibility of controlling the quantum coherence in single-electron devices. Subsequently, Qin *et al.*[23] showed that these coherent molecular states are robust even when coupled to acoustic phonons created in the system. The first observation of a coherent Kondo effect in a DQD was reported by Jeong *et al.*.[24] Indeed, the splitting of the Kondo resonance (into bonding and anti-bonding many-body states) was then clearly observed, as had been theoretically predicted.[11,12,19] However, no *single* Kondo peak has been experimentally observed to date, probably due to the small values of inter-dot tunnel coupling required, which leads to a very small overall conductance at half-filling.

In addition, several recent papers have been trying to determine under what experimental conditions it would be possible to observe manifestations of the NFL QCP mentioned above. In the theoretical side, Affleck *et al.*[25] have used bosonization to determine the energy scale below which the RG flows

to a FL QCP (away from the NFL QCP, as discussed above - see also Ref. 26). More importantly, an exact functional form for the conductance in the crossover region from NFL to FL was derived,[25] opening the doors for its possible experimental observation. Note that a very interesting experiment involving carefully approaching a Cobalt atom in an STM tip to another Cobalt atom laying on a gold surface has nonetheless failed to observe the NFL QCP physics.[27] Also, M. Lee *et al.* have found through NRG a conduction-band mediated superexchange J_I, which competes with the direct superexchange term $J_U = 4t^2/U$ and dominates for large values of U (intra-dot repulsion, and t being the inter-dot hopping matrix element). These two terms (related to inter-lead charge transfer) are known to destabilize the NFL QCP, by breaking parity. Indeed, as mentioned above,[6] this QCP is closely associated to the TCK fixed point which is believed to have been observed in only one system.[28] In a recent paper, F. W. Jayatilaka *et al.*,[6] using NRG, carefully analyze the experimental possibility of observing this QCP in a DQD.

In this work, we study the properties of a DQD (see Fig. 1) using the Slave Boson Mean Field Approximation (SBMFA) at finite U. The main property we are interested in is the behavior of the so-called *Kondo cloud* in a DQD. The Kondo cloud can be understood as the spatial region occupied by the conduction electrons that are collectively involved in screening the impurity spin.[29,30] In the case of the DQD analyzed here (Fig. 1), at half-filling, when the tunnel coupling between them is weak (as compared to the coupling of each QD to its adjacent lead), each QD will form its corresponding Kondo cloud with the conduction spins of the lead to which it is directly connected. However, as the inter-dot coupling increases, the system is driven through the crossover region between the Kondo regime and the antiferromagnetic 'molecular' regime. When passing through this region, the Kondo cloud associated to each dot should 'shrink' and disappear accordingly.

In a 1D system, the Kondo cloud is characterized by its length, which can be estimated by assuming that the mean free path of the many-body quasi-particle is related to a time scale associated to the Kondo temperature T_K. If one assumes that the electrons scattered by the single impurity propagate with the Fermi velocity v_F, the Kondo cloud length, ξ, is estimated as[29]

$$\xi \approx \frac{\hbar v_F}{k_B T_K}, \qquad (1)$$

where $\hbar$ and k_B are Planck and Boltzmann constants, respectively. Therefore, in the present case, it is important to determine whether for the DQD the Kondo cloud length also scales with the inverse of T_K, as shown in Eq. 1.

From a theoretical point of view, the Kondo cloud has been studied through different approaches.[31] The most common one is based on the study of the dependence of the spin-spin correlation with the distance between the impurity and the conduction electrons.[29] Using a variational approach it has been suggested that ξ does not play a significant role in the physics of a system of impurities in 2- and 3-dimensions.[32] However, the Kondo cloud is an important concept to analyze the conductance properties of 1-dimensional systems, like the one studied in this paper.

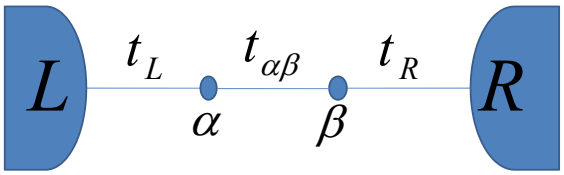

FIG. 1: (Color online) The figure sketches an artificial molecule consisting of two QDs with intra-dot Coulomb interaction U, and tunnel coupled to each other through the inter-dot matrix element $t_{\alpha\beta}$. In addition each QD is tunnel coupled to its adjacent metallic lead through the matrix element $t_{L(R)}$. The leads L and R act as charge reservoirs, being in thermodynamic equilibrium with the DQD.

Very recently, the authors studied the behavior of this correlation for arbitrary distances from a single impurity.[31] This study has been done by analyzing the effect of the Kondo resonance on the local density of states (LDOS) *away* from the impurity. Using this approach, it was possible to show that ξ behaves according to Eq. 1. As a consequence, it is in principle possible to determine T_K by studying the length of the associated Kondo cloud.

To be more precise, the main objective of this paper is to answer the question: *how does the Kondo temperature and the Kondo cloud depend on the parameters of the DQD?* To this end, we employ the finite-U SBMFA, which requires a more involved numerical calculation than the infinite-U SBMFA,[11,16] and therefore eliminates the misconceptions created by the artificial introduction of an extra antiferromagnetic inter-dot interaction J in the Hamiltonian. We also study the system at finite temperature and estimate T_K by associating it to the temperature above which the width of the Kondo peak in the LDOS vanishes. In this limit, within this approximation, the QDs decouple from the rest of the system. We then compare the Kondo temperature obtained from the length of the Kondo cloud with the one obtained from the slave-boson criterion just described above. The results agree very well in the region of parameter space where the system is in the Kondo regime.

The paper is organized as follows: In Sec. II we present the model for the DQD and describe the finite-U SBMFA, while in Sec. III we present SBMFA results at half-filling. Sec. IV is dedicated to the study of the Kondo cloud inside the leads, presenting a way of calculating its extension and from it the Kondo temperature. In Sec. V we compare the results obtained for T_K from the calculation of the Kondo cloud extension with those obtained by calculating the width of the Kondo peak at finite temperature. In Sec VI we present our conclusions, and relegate to the Appendix some more technical results.

II. MODEL AND SLAVE BOSON MEAN FIELD APPROACH

The system of two quantum dots presented in the Fig. 1 is described by an Anderson Hamiltonian which can be separated in three parts, $H = H_0 + H_t + H_{leads}$, where

$$H_0 = \sum_{\substack{i=\alpha,\beta \\ \sigma}} \epsilon_i c^\dagger_{i\sigma} c_{i\sigma} + \sum_{i=\alpha,\beta} U c^\dagger_{i\uparrow} c^\dagger_{i\downarrow} c_{i\downarrow} c_{i\uparrow} \quad (2)$$

describes the isolated QDs, in which $c^\dagger_{i\sigma}$ ($c_{i\sigma}$) creates (annihilates) an electron with energy ϵ_i and spin σ in the ith QD ($i = \alpha,\ \beta$), and the second term corresponds to the Coulomb interaction U in each QD.

$$H_t = \sum_\sigma \left(t_L c^\dagger_{-1\sigma} c_{\alpha\sigma} + t_R c^\dagger_{1\sigma} c_{\beta\sigma} + H.c. \right) + \sum_\sigma t_{\alpha\beta} \left(c^\dagger_{\alpha\sigma} c_{\beta\sigma} + H.c. \right) \quad (3)$$

describes the connection of each QD with its adjacent lead (first term) and the tunnel coupling between the QDs (second term). Finally,

$$H_{leads} = t \sum_{\substack{i=1 \\ \sigma}}^{\infty} \left(c^\dagger_{i\sigma} c_{i+1\sigma} + c^\dagger_{-i\sigma} c_{-i-1\sigma} + H.c. \right) \quad (4)$$

describes the leads, modeled as two semi-infinity tight-binding chains of non-interacting sites connected through the hopping term t. For simplicity, we take the applied gate potential to be equal in both QDs, i.e., $\epsilon_\alpha = \epsilon_\beta = V_g$, and we consider symmetric coupling to the leads, $t_L = t_R = t'$. Hereafter, we choose $t = 1$ as our energy unit and set $\hbar = k_B = 1$.

Within the slave boson formalism, the physics underlying the Kondo regime is brought into the model by the introduction of the auxiliary bosons e_i, $p_{i\sigma}$, and $d_{i\sigma}$, which project the Hilbert space onto space sectors with zero, one, and two electrons, respectively. To accommodate the new bosonic field with these operators, the Hilbert space is naturally enlarged, and the single electron operator $c_{i\sigma}$ ($c^\dagger_{i\sigma}$) is replaced by a quasi-electron operator $Z c_{i\sigma}$ ($Z^\dagger c^\dagger_{i\sigma}$), where the Z-operator, in mean field approximation becomes just a real factor[33]

$$Z_{i\sigma} = [1 - \langle d_i \rangle^2 - \langle p_{i\sigma} \rangle^2]^{-1/2} (\langle e_i \rangle \langle p_{i\sigma} \rangle + \langle p_{i\sigma} \rangle \langle d_i \rangle) \times \times [1 - \langle e_i \rangle^2 - \langle p_{i\bar{\sigma}} \rangle^2]^{-1/2}, \quad (5)$$

where i denotes the ith QD and $\langle e_i \rangle$, $\langle p_{i\sigma} \rangle$, and $\langle d_{i\sigma} \rangle$ the mean value of the slave boson operators. The full Hilbert space has to be restricted to the physically meaningful sector by imposing the constraints

$$\langle e_i \rangle^2 + \sum_\sigma \langle p_{i\sigma} \rangle^2 + \langle d_i \rangle^2 - 1 = 0, \quad (6)$$

and

$$n_{i\sigma} - \langle p_{i\sigma} \rangle^2 - \langle d_i \rangle^2 = 0, \quad (7)$$

via Lagrange multipliers $\lambda^{(1)}_i$ and $\lambda^{(2)}_{i\sigma}$. Considering the hybridization of the fermion operators in H_0 and H_t, and also introducing the Lagrange multipliers λ^i_1 and $\lambda^i_{2\sigma}$, we can write, the effective Hamiltonian as,

$$\begin{aligned} H_{eff} = & \sum_{\substack{i=\alpha,\beta \\ \sigma}} \tilde{\epsilon}_i n_{i\sigma} + \sum_{\substack{i=L(j=\alpha), \\ R(j=\beta)}}^{\sigma} t_i Z \left[c^\dagger_{i\sigma} c_{j\sigma} + H.c. \right] + \\ & + \sum_{i=\alpha,\beta} U_i \langle d_i \rangle^2 + \sum_\sigma t_{\alpha\beta} Z^2 \left[c^\dagger_{\alpha\sigma} c_{\beta\sigma} + H.c. \right] + \\ & + \sum_{i=\alpha,\beta} \lambda^i_1 \left[\langle e_i \rangle^2 + \sum_\sigma \langle p_{i\sigma} \rangle^2 + \langle d_i \rangle^2 - 1 \right] + \\ & - \sum_{\substack{i=\alpha,\beta \\ \sigma}} \lambda^i_{2\sigma} \left[\langle p_{i\sigma} \rangle^2 + \langle d_i \rangle^2 \right] + H_{leads}, \end{aligned} \quad (8)$$

where $\tilde{\epsilon}_i = \epsilon_i + \lambda^i_{2\sigma}$ is the renormalized quasi-fermion energy. It is important to notice that the replacement of the single-fermion operator, in mean-field approximation, results to be equivalent to a renormalization of the connections t' and $t_{\alpha\beta}$ by a multiplicative parameter Z and Z^2, respectively. With the effective Hamiltonian H_{eff} we can obtain the free energy of the system, which is minimized with respect to each component of the set of parameters,

$$\gamma = \{e_\alpha, e_\beta, p_{\alpha\sigma}, p_{\beta\sigma}, d_\alpha, d_\beta, \lambda^\alpha_1, \lambda^\beta_1, \lambda^\alpha_{2\sigma}, \lambda^\beta_{2\sigma}\}. \quad (9)$$

The minimization of the free energy provides a set of non-linear equations that has to be solved in a self-consistent way. See Appendix B for details.

III. DIFFERENT MANY-BODY REGIMES

In this section, we present SBMFA numerical results for the low-temperature physics of the DQD shown in Fig. 1. These results were obtained in the two different regions of the parameter space, as described in the Introduction, and allow the analysis of transport properties in the two well characterized quantum states of the DQD, as well as in the crossover region between them. In addition, some results for the molecular Kondo regime, which is characterized by an effective Coulomb interaction U_{eff}, will be presented as an Appendix.

A. Atomic Kondo Regime at Half-Filling

To start the discussion concerning the different regimes of the system and the crossover between them, we present in Figs. 2, 3, and 4 the renormalized energy level $\tilde{\epsilon}_{\alpha(\beta)}$ and the local density of states (LDOS) of the QDs, the conductance G, and the renormalization parameter Z^2, respectively. All these quantities (except for the LDOS in Fig. 2(B) are calculated as a function of the gate potential V_g and for different values of $t_{\alpha\beta}$, and $E_F = 0$ in both reservoirs. If the gate potential satisfies $V_g \approx -U/2$ (i.e., the DQD is occupied by two electrons), then, for small values of $t_{\alpha\beta}$, the system is expected to

be in the Kondo regime resulting from the singlet state created by the antiferromagnetic correlation of each QD with the conduction electron spins of the corresponding lead. The formation of this Kondo state is characterized by the plateau structure, around $V_g = -U/2$, at the Fermi level, observed in the results in Fig. 2(A) for $t_{\alpha\beta} = 0.025$, for example. This plateau is related to the opening of a conducting channel (at $\omega = 0$), which allow charge transport through the DQD. Associated with this conduction channel there is a Kondo resonance at the Fermi level, which can be clearly seen in Fig. 2(B) [(black) square curve, for $t_{\alpha\beta} = 0.025$], which shows results for the QDs' local density of states (LDOS) close to the Fermi level for $V_g = -U/2$. Note that the Kondo peak is split (and suppressed) for the smallest value of $t_{\alpha\beta} = 0.025$ in Fig. 2(B), and that this splitting becomes more pronounced as $t_{\alpha\beta}$ increases.[34] Consequently, the conductance (shown in Fig. 3) is also suppressed from its maximum value $G = G_0$ at $V_g = -U/2$. As mentioned in section II, another important characteristic of the Kondo regime, in the finite-U slave boson approach, is the renormalization of the couplings through the parameter Z (between both QDs and between each QD and its adjacent lead), as shown in Fig. 4. Note that for $t_{\alpha\beta} = 0.025$ [(black) square curve], this renormalization is the strongest. This result shows a large reduction of the parameter Z, reaching $Z \approx \sqrt{0.05} \approx 0.22$, strongly suppressing the renormalized hoppings t' and $t_{\alpha\beta}$, by factors Z and Z^2, respectively [see eq. (8)]. This is an indication of the formation of a Kondo state, where spin fluctuations are enhanced and charge fluctuations in the QDs are suppressed, which is reflect in the decrease of the effective hoppings connecting the QDs to each other and to the leads. One should remark that the split Kondo peak [(black) square curve] in Fig. 2(B) is associated to the many-body coherent states which had been theoretically predicted[11,12,19] and experimentally observed.[24]

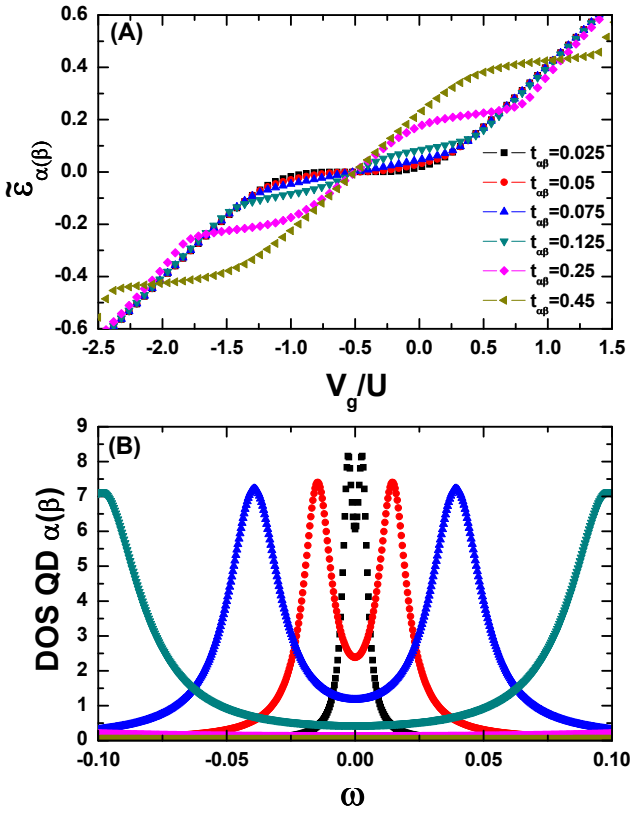

FIG. 2: (Color online) (A) behavior of the renormalized local energy state $\tilde{\epsilon}_{\alpha(\beta)}$ of the QDs as a function of the gate potential V_g. The parameters used are $U = 0.5$, $t' = 0.15$, Fermi energy $E_f = 0$, and with different magnitudes for $t_{\alpha\beta}$ (see legend). As $t_{\alpha\beta}$ increases, the plateau observed at $\tilde{\epsilon}_{\alpha(\beta)} = 0$, characteristic of the Kondo regime, is gradually suppressed. Note that for the largest value of $t_{\alpha\beta} = 0.45$ one has now two plateaus located at $\tilde{\epsilon}_{\alpha(\beta)} \approx \pm t_{\alpha\beta}$, which (as noted in Appendix A) are associated to the molecular Kondo regimes at quarter-filling. (B) QD's LDOS for $V_g = -U/2$, and the same $t_{\alpha\beta}$ values as in panel (A). For the smallest value of $t_{\alpha\beta} = 0.025$ [(black) squares curve) a splitting of the Kondo resonance is already observed. Note that for $t_{\alpha\beta} = 0.125$ [(green) down-triangles curve], the separation between the peaks is already close to $2t_{\alpha\beta}$, which is the separation expected for single-particle molecular orbitals, as mentioned in the Introduction.

B. Molecular Regime at Half-Filling

With the gradual increase in the magnitude of the connection $t_{\alpha\beta}$, an antiferromagnetic interaction $J = {t_{\alpha\beta}}^2/U$ develops between the spins localized in each QD, competing with the Kondo state and, for large values of $t_{\alpha\beta}$, it is responsible for the total suppression of the Kondo state at half-filling. From Fig. 2(A) we note the progressive destruction, as $t_{\alpha\beta}$ increases, of the plateau in the $\tilde{\epsilon}_{\alpha(\beta)}$ vs V_g curves, around half-filling. Simultaneously, it is possible to observe the development of two other plateaus, for $V_g/U > 0$ and $V_g/U < -1$, that correspond to the emergence of one- and three-electron Kondo regimes, respectively, which will be discussed in Appendix A. In Fig. 2(B) (where $V_g = -U/2$, i.e., particle-hole symmetric point), the transition to the molecular regime, accompanied by the destruction of the Kondo resonance [(black) squares curve), and the formation of the molecular antiferromagnetic state [(blue) triangle curve) is reflected in the LDOS $\rho_{\alpha(\beta)}$ of the QDs. Note in Fig. 2(B) that for $t_{\alpha\beta} = 0.125$ [(green) down-triangle curve], the separation between the peaks is already $\approx 2t_{\alpha\beta}$, indicating that these peaks are associated to the coherent single-particle molecular states, as experimentally observed in Refs. 21–23. The transition to the molecular regime can also be observed in Fig. 4, showing that the renormalization of the dot hopping connections is reduced, as the renormalization parameter rapidly approaches the value $Z \approx 1.0$ as $t_{\alpha\beta}$ increases. This effect is reflected in the conductance of the system as presented in Fig. 3, which is strongly suppressed at half-filling for larger values of $t_{\alpha\beta}$. The plateaus outside the half-filling regime shown in Fig.2(A), for the largest values of $t_{\alpha\beta}$ correspond to the conductance of the DQD at the molecular one- and three-Kondo regime that, as mentioned, are discussed in Appendix A.

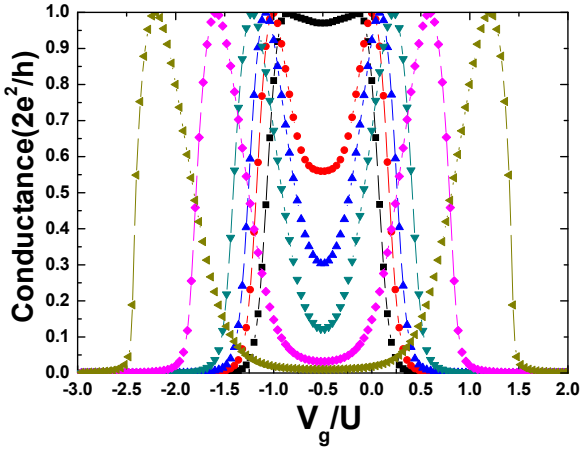

FIG. 3: (Color online) Conductance as a function of V_g for $t_{\alpha\beta} = 0.025$ [(black) squares curve], $t_{\alpha\beta} = 0.05$ [(red) circles], $t_{\alpha\beta} = 0.075$ [(blue) up-triangles], $t_{\alpha\beta} = 0.125$ [(green) down-triangles], $t_{\alpha\beta} = 0.25$ [(magenta) diamonds] and $t_{\alpha\beta} = 0.45$ [(light green) left-triangle]. The other parameters are $t' = 0.15$ and $U = 0.5$.

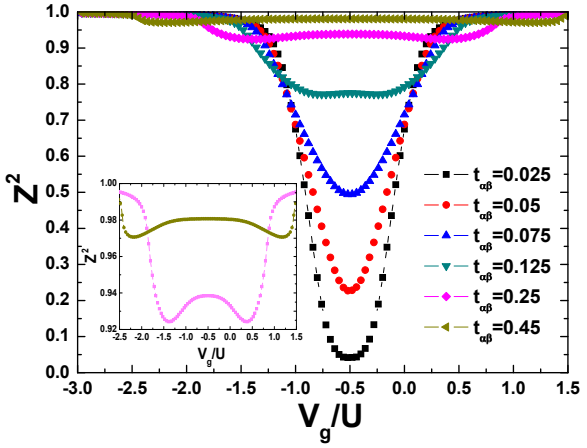

FIG. 4: (Color online) Renormalization parameter Z^2 as a function of V_g for the same $t_{\alpha\beta}$, U, and t' values as in Fig. 3. The inset shows the small renormalization of Z characteristic of the molecular Kondo regime.

IV. KONDO CLOUD

A. Cloud Extension Function

In this section we introduce a new perspective to the Kondo problem in a strongly coupled DQD at half-filling, based on the analysis of the extension of the Kondo cloud inside the metallic leads. To analyze the extension of the Kondo cloud we use the method developed in Ref. 31, where the authors analyze the propagation into the leads (away from the QD) of the perturbation in the LDOS, introduced by the Kondo resonance *at* the QD. To study this propagation, a function $F(N)$ was defined, which quantifies the perturbation produced by the presence of the Kondo cloud in the Nth site of the lead (counted from the border of the semi-infinity chain). In the current work we consider a similar expression,

$$F(N) = \int_{-\infty}^{+\infty} [\rho_N^k(\omega) - \rho_N^{nk}(\omega)]\rho_{\alpha(\beta)}(\omega)d\omega, \qquad (10)$$

to quantify this perturbation. Instead of using a Gaussian function with width T_K to convolute the density of states and eliminate the Friedel oscillations,[30] allowing the study of the region near the Fermi level, we use the LDOS $\rho_{\alpha(\beta)}$ of the QD. Note that, as $\rho_\alpha = \rho_\beta$, we will omit the subscripts α and β from the rest of the equations in this subsection. The use of this definition for the convolution function (ρ) has the advantage of directly incorporating into $F(N)$ the physical information associated with the Kondo ground state. In this expression, ρ_N^k and ρ_N^{nk} represent the LDOS calculated in the Nth site inside the lead (L or R) with the system *in* and *away from* the Kondo regime, respectively. The last condition is enforced by disconnecting the DQD from the leads, i.e., by calculating the LDOS for $t' = 0$. It is well known that, within the SBMFA, this is equivalent to taking the system to a temperature $T > T_K$.[10,16]

The LDOS appearing in the integrand of $F(N)$ is proportional to the imaginary part of the Green's function G_{NN} defined at the N^{th} site inside the semi-infinite metallic leads. Considering the left lead, for instance, we can write

$$G_{NN} = g_{NN} + g_{N1}t'G_{\alpha N}. \qquad (11)$$

In this expression g_{NN} is defined as the Green's function at site N of the left lead when $t' = 0$ and g_{N1} satisfies the equation

$$g_{N1} = t^{N-1}\tilde{g}_L^N, \qquad (12)$$

where

$$\tilde{g}_L = \frac{\omega - \sqrt{\omega^2 - 4t^2}}{2t^2} \qquad (13)$$

is the Green's function defined for the left lead. For $G_{\alpha N(N\alpha)}$ we have

$$G_{\alpha N} = G_{N\alpha} = g_{N1}t'G_{\alpha\alpha}, \qquad (14)$$

where $G_{\alpha\alpha}$ is the dressed function at the QD α. Substituting $G_{\alpha N}$ into eq. (11), yields

$$G_{NN} = g_{NN} + t'^2(g_{N1})^2G_{\alpha\alpha}. \qquad (15)$$

We note that the Kondo physics is introduced into G_{NN} through the term proportional to t'^2. The imaginary part of this function is proportional to the LDOS ρ_N^k at the N^{th} site. The non-Kondo solution is obtained by eliminating the effects resulting from the presence of the QD by considering $t' = 0$ in the expression of G_{NN}. So, ρ_N^{nk} is defined as $\rho_N^{nk} = -(1/\pi)\mathtt{Im}\, g_{NN}$.

Considering the analytical expression for ρ_N^k and ρ_N^{nk} we obtain

$$\rho_N^k - \rho_N^{nk} = -\frac{1}{\pi}\mathtt{Im}[t'^2(g_{N1})^2G_{\alpha\alpha}]. \qquad (16)$$

Substituting g_{N1} into eq. (16) we obtain

$$\rho_N^k - \rho_N^{nk} = -\frac{1}{\pi}\mathtt{Im}[t'^2\tilde{g}_L^{2N}t^{2N-2}G_{\alpha\alpha}]. \quad (17)$$

This expression, when substituted into eq. (10), results in

$$F(N) = -\frac{1}{\pi}\int_{-\infty}^{+\infty}\mathtt{Im}[t'^2\tilde{g}_L^{2N}t^{2N-2}G_{\alpha\alpha}(\omega)]\rho(\omega)d\omega, \quad (18)$$

where all the effects of strong correlation present at site N are contained in the Green's function of the QDs. Note that when $t_{\alpha\beta} = 0$ one should obtain the results from previous calculations for a single-QD Kondo cloud.[31] For finite $t_{\alpha\beta}$, the competition between Kondo and antiferromagnetism is contained in $G_{\alpha\alpha}(\omega)$, and therefore should be reflected in $F(N)$.

B. LDOS

The LDOS ρ_N^k and ρ_N^{nk}, calculated at the site $N = 50$ of the leads, for the system with $t_{\alpha\beta} = 0$, are shown in Fig. 5. As in the rest of this paper, the results presented in this figure were obtained for $V_g = -U/2$, $U = 0.5$, and $t' = 0.2$. The LDOS ρ_N^{nk} was calculated for an isolated lead ($t' = 0$). The Kondo resonance at the QD is shown in the (blue) triangle curve of Fig. 5. On the other hand, the LDOS $\rho_{N=50}^k$ [(red) circle curve] shows a small peak at the Fermi level. The presence of this peak is a sign of the Kondo resonance 'propagating' through the sites of the leads and reflects the existence of the Kondo cloud, with an extension ξ, dependent on the Kondo temperature T_K. In our context, the extension of the Kondo cloud is obtained from $F(N)$ (see next section for more details). It is important to note here that the propagated Kondo peak along the leads appears as a resonance or an antiresonance depending on whether the site N is even or odd, respectively.[31]

Figure 6 shows the behavior of the LDOS for different values of $t_{\alpha\beta}$, illustrating how the competition between the Kondo regime and the antiferromagnetic correlation manifests itself in the LDOS at an arbitrary site ($N = 50$). The (magenta) dashed curve is the LDOS for a lead with no connection to the dots, which, as a reference, corresponds to the expected result obtained for a non-Kondo regime. The (black) down-triangle curve corresponds to $t_{\alpha\beta} = 0$ ($t' = 0.2$) and shows the characteristic Kondo resonance propagated to $N = 50$. It is clear from the figure that an increase of the tunnel coupling $t_{\alpha\beta}$ drives the system from a Kondo regime to a non-Kondo ground state, as the LDOS at (and around) the Fermi level is clearly suppressed, approaching the value for the disconnected DQD [(magenta) dashed curve].

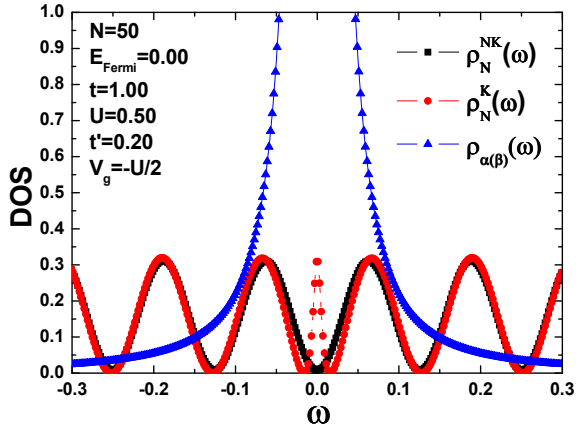

FIG. 5: (Color online) The figure shows the effect produced by the presence of the impurity $\alpha(\beta)$ in the LDOS calculated at the site $N = 50$ [inside the lead L(R)]. The (black) squares curve shows the LDOS (at site $N = 50$) for the isolated lead; the (red) circles curve shows the LDOS when each lead is connected to its respective QD, for $t_{\alpha\beta} = 0$; and the (blue) triangles curve shows the LDOS for the impurity.

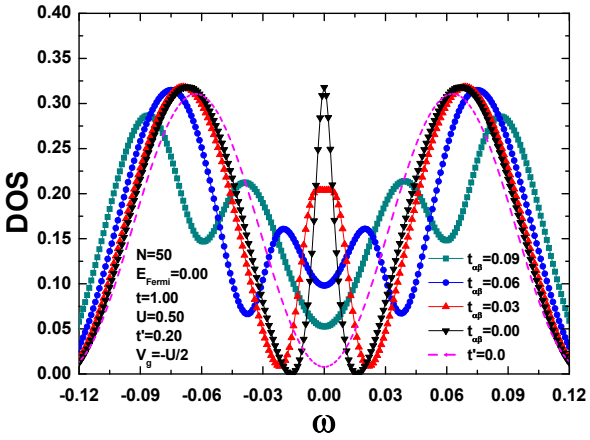

FIG. 6: (Color online) The figure shows the effect produced by the antiferromagnetic interaction $J = 4t_{\alpha\beta}^2/U$ between the QDs in the LDOS at site $N = 50$ inside the leads. The (black) down-triangle curve shows the LDOS calculated at $N = 50$ for $t_{\alpha\beta} = 0$. The (red) up-triangles, (blue) circles, and (cyan) down-triangles curves are obtained for $t_{\alpha\beta} = 0.03$, $t_{\alpha\beta} = 0.06$, and $t_{\alpha\beta} = 0.09$, respectively. The (magenta) dashed curve shows the LDOS for the isolated leads ($t' = 0$). The other parameters are $V_g = -U/2$, $U = 0.5$, and $t' = 0.2$.

V. KONDO TEMPERATURE

A. Kondo Temperature from the Cloud Extension Function

Figure 7 shows the logarithmic dependence of the function $F(N)$ for various inter-dot couplings $t_{\alpha\beta}$. Differently from the result obtained for a system of one QD connected to a metallic lead,[31] this function presents now an oscillatory behavior with a frequency associated to the inter-dot coupling. However, similarly to the single-QD case, the extension ξ of the Kondo cloud can still be obtained, in this case by the exponential decay of its envelop function. The physical information contained in this function is extracted from the straight lines, tangent to the logarithm of the $F(N)$ function. Specifically, the extension of the Kondo cloud, as a function of the

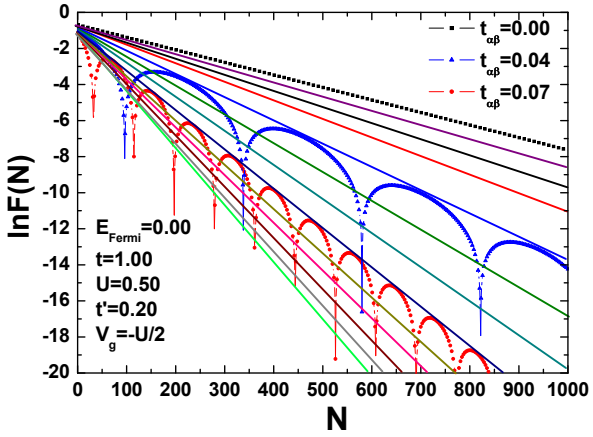

FIG. 7: (Color online) Natural logarithm of the cloud extension function F *vs* the distance N (from the border of the semi-infinite chain) for $t_{\alpha\beta} = 0.0$ [(black) squares], $t_{\alpha\beta} = 0.04$ [(blue) triangles], and $t_{\alpha\beta} = 0.07$ [(red) circles]. The straight lines are tangents to lnF and correspond to $t_{\alpha\beta} = 0.01$ [(purple) line], $t_{\alpha\beta} = 0.02$ [(black) line], $t_{\alpha\beta} = 0.03$ [(red) line], ..., $t_{\alpha\beta} = 0.12$ [(green) line]. The other parameters are $V_g = -U/2$, $U = 0.5$, and $t' = 0.2$.

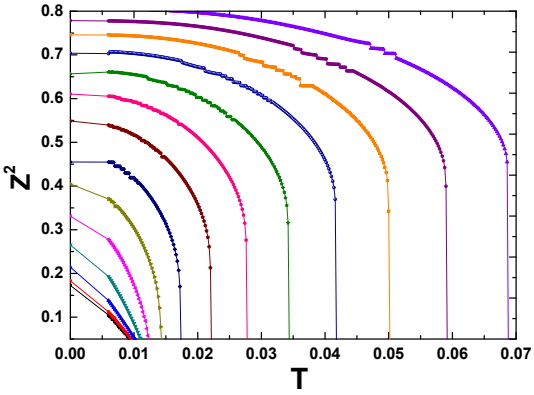

FIG. 8: (Color online) Renormalization parameter Z^2 as a function of temperature T for values of $t_{\alpha\beta}$ ranging from 0.00 [(black) leftmost curve] to 0.13 [(purple) rightmost curve]. The other parameters are $t' = 0.2$, $U = 0.5$, $V_g = -U/2$, and $E_f = 0.0$.

inter-dot connection, can be obtained from the slopes of these lines, which are proportional to $1/\xi$ (see eq. (23) in Ref. 31).

In Fig. 7 we show the function $\ln F(N)$ for $t_{\alpha\beta} = 0$ [(black) squares curve], $t_{\alpha\beta} = 0.04$ [(blue) triangles curve], and $t_{\alpha\beta} = 0.07$ [(red) circles curve], as well as their respective tangent lines. For intermediate values of $t_{\alpha\beta}$ we present only the tangents to $\ln F(N)$. As mentioned above, the slopes of these straight lines are proportional to $1/\xi$ and allow us to obtain the Kondo temperature through the expression $\xi = \frac{\Gamma}{T_K}$, proposed in Ref. 31. The values obtained for the Kondo temperature T_K are presented in the (red) circles curve in Fig. 9, as function of $t_{\alpha\beta}$ (we label it as T_K^{KC}, i.e., the Kondo temperature obtained through the extension of the Kondo cloud). We note that, for $\frac{4t_{\alpha\beta}^2}{U} < T_K$, which implies $t_{\alpha\beta} < 0.07$, T_K presents an exponential behavior, in accordance with results obtained by Aono and Eto[11] using a slave boson formalism with an infinite Hubbard U.

B. Kondo Temperature in the Finite Temperature SBMFA

In this section we determine the Kondo temperature T_K of the DQD by extending the slave boson formalism for finite temperature. In this formalism, the impurity is decoupled from the rest of the system for a critical temperature T_c. Although phase transitions are typical artifacts of mean field solutions, the temperature for which this decoupling occurs can be considered as a reasonable approximation to the Kondo temperature, which physically corresponds to a crossover between two regimes. The decoupling occurs through the parameter Z, which renormalizes the coupling of the QDs to the leads, $\tilde{t'} = Zt'$ and $\tilde{t_{\alpha\beta}} = Z^2 t_{\alpha\beta}$, which is vanishingly small when $T \approx T_K$. The parameter Z, as a function of temperature, is studied in Fig. 8, for various values of $t_{\alpha\beta}$. We see from this result that the parameter Z^2 vanishes rapidly when the temperature approaches the characteristic value T_c.

The values of T_c obtained for the different values of $t_{\alpha\beta}$ are represented by the square (black) curve in the Fig. 9 (we label it T_K^{Cut}), and it agrees with the values obtained for T_K^{KC} from the function $\ln F(N)$ associated to the extension of the Kondo cloud in the metallic leads. We observe a qualitative and semiquantitative agreement between these two ways of calculating the Kondo temperature, giving support to the interpretations we are proposing. We note that increasing $t_{\alpha\beta} > 0.07$ the values of T_c become increasingly different from the T_K values obtained from the extension of the Kondo cloud. These are precisely values for which ${t_{\alpha\beta}}^2/U > T_K$, and the discrepancy starts at $t_{\alpha\beta} \gtrsim 0.07$, where the DQD enters a crossover region which extends up to values of $t_{\alpha\beta}$ for which $4t_{\alpha\beta}^2/U > 2T_K^{(0)}$, where the DQD enters into an antiferromagnetic phase ($T_K^{(0)}$ is the Kondo temperature of each QD when $t_{\alpha\beta} = 0.0$), according to previous works (see Ref. 11 and references therein).

VI. CONCLUSIONS

In this paper, the interplay between the antiferromagnetic interaction and the Kondo effect for a DQD at half-filling has been studied in detail. In particular, we have analyzed the dependence of the extension of the Kondo cloud on the inter-dot tunnel coupling ($t_{\alpha\beta}$) when the system is driven from the half-filling Kondo regime to the antiferromagnetic molecular ground state, as $t_{\alpha\beta}$ increases. The extension of the Kondo cloud and its associated T_K were obtained by analyzing the propagation inside the leads of the Kondo resonance 'originating' at the dots. In the Kondo regime, the T_K results obtained through the Kondo cloud extension were almost identical to the 'Kondo transition temperature' T_c obtained from the finite-temperature extension of the MFSBA. Although we know that the decoupling of the DQD from the leads (occurring at T_c) is an artifact of the MFSBA, our results confirm

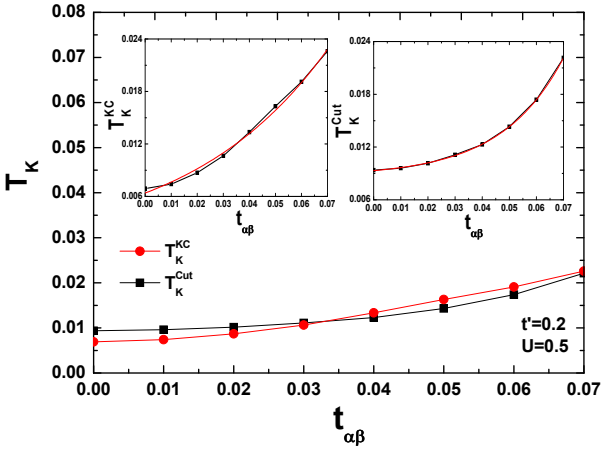

FIG. 9: (Color online) Kondo temperature T_K^{KC} and T_K^{Cut} as a function of $t_{\alpha\beta}$. The (red) circles curve corresponds to T_K obtained from the extension ξ of the Kondo cloud, while the (black) squares curve corresponds to T_K as obtained through the critical temperature T_c for which the QD's are decoupled (see text), with $Z \to 0$. The insets show the exponential fits obtained for each T_K in the region where the system is expected to be in the Kondo regime. The values for the other parameters are $V_g = -U/2$, $U = 0.5$, and $t' = 0.2$.

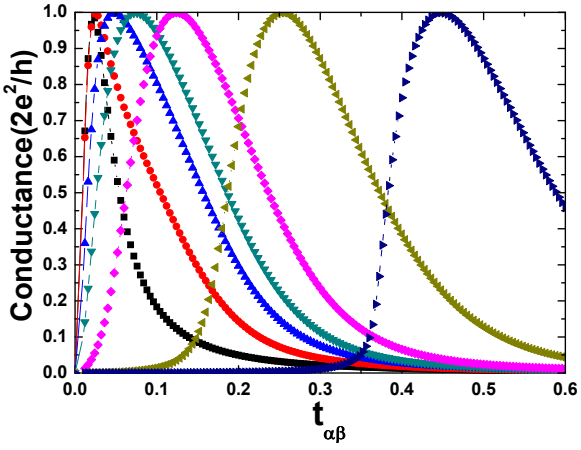

FIG. 10: (Color online) Conductance as a function of $t_{\alpha\beta}$ for $V_g/U = -0.5$ [(black) squares], $V_g/U = -0.14$ [(red) circles], $V_g/U = 0.0$ [(blue) up-triangles], $V_g/U = 0.08$ [(cyan) down-triangle], $V_g/U = 0.22$ [(magenta) diamond], $V_g/U = 0.6$ [left-triangle (gold)] and $V_g/U = 1.2$ [(royal) right-triangle]. The other parameters are $t' = 0.15$ and $U = 0.5$.

that the T_c can be reliably taken to be $\approx T_K$ in a DQD, very much in the same way as in the case of one impurity. Note that the dependence of T_k obtained by both approaches agrees with previous results by Aono and Eto.[11]

The study of the Kondo regime in the DQD was done within the context of a finite U treatment. As U is finite, the Hamiltonian incorporates the correlation between the QD's spins. This allows us to avoid introducing an artificial antiferromagnetic interaction between the QD's, normally incorporated in $U = \infty$ approaches (as done, for example, in Ref. 16), which provides more confidence to our results. Its important to note that the study developed in this paper opens a set of conceptual ideas that can be useful to understand the effects of the RKKY interaction between two QD's located at an arbitrary distance between themselves, as well as the transport associated to them.

Appendix A: Molecular Kondo Regime at Quarter-Filling

Given the importance in a DQD, as mentioned in the Introduction, of the concept of molecular states (or molecular orbitals), the authors will briefly describe the properties of the molecular orbitals in a DQD, as done previously for related systems.[35] For recent work by some of the authors, see References 36,37. A system of two or more coupled QDs is said to be in the molecular regime when the charge transport occurs through orbitals that involve linear combinations of levels in each QD (which could be called 'atomic' orbitals). The molecular Kondo effect occurs when an unpaired spin residing in a molecular orbital is screened by conduction electrons.[37] It is clear that, in the molecular Kondo regime, the charge at each QD in a multi-QD system does not correspond to an integer value. As a consequence, the non-integer QD charge ground state of a multi-QD structure cannot be used as a criterion to identify the system as being in a fluctuating valence regime, as it could be in a molecular Kondo ground state, involving more than one QD. The determination of the real nature of the ground state of these systems requires a careful analysis, mainly for parameter values where the system is in a transition between the molecular and the atomic regimes.

In the case here analyzed for a DQD, by adjusting V_g to have one (or three) total number of electrons in the DQD, and considering relatively large values of $t_{\alpha\beta}$, the quarter-filled molecular Kondo regime is accessed. In the context of the finite-U slave boson formalism, this regime is characterized by two plateau structures in $\tilde{\epsilon}_{\alpha(\beta)}$ [as observed at half-filling in Fig. 2(A)] at $\tilde{\epsilon}_{\alpha(\beta)} = \pm t_{\alpha\beta}$. The formation of these plateaus is associated with two new resonances which allow charge transport through the DQD, as can be seen by the well separated double peaks in the conductance in Fig. 3 [(yellow) left-triangle and (magenta) diamond curves, for $t_{\alpha\beta} = 0.45$ and 0.25, respectively].

Figure 4 shows that as the system is driven out of the Kondo regime, at $V_g = -U/2$, by increasing $t_{\alpha\beta}$, the parameter $Z \to 1.0$, thus eliminating the renormalization of the hopping matrix elements [see eq. (8)]. As an important characteristic of this result, we note two small suppressions of Z^2 for the (yellow) left-triangle and (magenta) diamond curves in the one- and three-electron regions of V_g. This region is amplified in the inset of Fig. 4 and reflects a small renormalization provided by the Z parameter, characteristic of the molecular Kondo regime.

To investigate in more detail the effect of the different regimes in the transport properties of the DQD, in Fig. 10 we present the conductance as a function of $t_{\alpha\beta}$ for different values of V_g. These results are fitted by the analytic expression

$$f(t_{\alpha\beta}) = \frac{4\Gamma^2 t_{\alpha\beta}^2}{(\Gamma^2 + t_{\alpha\beta}^2 - \tilde{\epsilon}_i^2)^2 - 4\tilde{\epsilon}_i^2\Gamma^2}, \qquad \text{(A1)}$$

where $\Gamma = \pi t_{L(R)}^2 \rho(E_F)$ is the coupling constant and $i = \alpha(\beta)$. This expression is an extension of the one obtained by Georges and Meir[16] and is valid also away from the particle-hole symmetric point, $V_g = -U/2$. Exactly at $V_g = -U/2$, the DQD has one electron in each QD and the conductance is maximum when $t_{\alpha\beta} = \Gamma$. For higher values of $t_{\alpha\beta}$, as V_g moves away from $-U/2$, the DQD approaches the quarter filling molecular Kondo regime. This occurs when the charge of the system is nearly one ($n_\alpha + n_\beta \approx 1$) or three electrons ($n_\alpha + n_\beta \approx 3$). This regime in the conductance is reflected in Fig. 3 by the two peaks which occur near the region of one and three electron occupation. Figure 10 shows the conductance as function of $t_{\alpha\beta}$ for various values of V_g, that correspond to the positions of the conductance peaks in Fig. 3 (for $V_g \geq -U/2$). From the results obtained for $V_g > 0$ one can identify two crossover regions for each V_g as $t_{\alpha\beta}$ increases: one corresponding to the transition from an empty dot situation to a molecular Kondo regime, with an increasing conductance region and the other, for values of $t_{\alpha\beta}$ above the maximum of the conductance, corresponding to the antiferromagnetic molecular regime where the conductance decreases, and the DQD's occupancy increases.

To better understand the physics underlying the strong coupled QDs in the transition region between the different regimes in the parameter space defined by $t_{\alpha\beta}$ and V_g, we use the exact solution obtained in Appendix D, when the QDs are disconnected from their leads. We obtain that $E_0^{(1e)} = \epsilon_0 - t_{\alpha\beta}$ and $E_0^{(2e)} = 2\epsilon_0 + \frac{U - \sqrt{U^2 + 16t_{\alpha\beta}^2}}{2}$ are the lowest energies in the one- and two-electron sector, respectively. Considering these expressions in a situation in which the charge occupation is increasing, we conclude that the inclusion of an extra electron into the DQD requires an extra energy given by, $E_0^{(2e)} - 2E_0^{(1e)} = 2t_{\alpha\beta} + \frac{U - \sqrt{U^2 + 16t_{\alpha\beta}^2}}{2}$. This extra energy can be identified with an *effective Coulomb* interaction

$$U_{eff} \;=\; 2t_{\alpha\beta} + \frac{U - \sqrt{U^2 + 16t_{\alpha\beta}^2}}{2}, \qquad \text{(A2)}$$

which, for small values of $U/t_{\alpha\beta}$, is $\approx U/2 + \mathcal{O}\left(U^2/16t_{\alpha\beta}\right)$. The addition of a second electron in the DQD is achieved by adjusting the gate potential V_g. In fact, for $V_g \approx t_{\alpha\beta} - U/2$, the DQD is basically double occupied, characterizing a transition from a molecular Kondo regime (at quarter-filling) to an antiferromagnetic state, or to a two-impurity half-filling Kondo regime, depending upon the ratio T_K/J being less or greater than unity, respectively.

Appendix B: The minimization of the free energy in the SBMFA

The free energy of the DQD is given by

$$F(\gamma_l) \;=\; -k_B T \ln\left[\sum_i e^{-\beta E_i(\gamma_l)}\right], \qquad \text{(B1)}$$

where $\beta = 1/k_B T$, and γ_l denotes the Lagrange multipliers. Differentiating F with respect to γ_l we obtain

$$\begin{aligned}\frac{\partial F}{\partial \gamma_l} &= \beta T k_B \frac{\sum_i \frac{\partial E_i(\gamma_l)}{\partial(\gamma_l)} e^{-\beta E_i(\gamma_l)}}{\sum_i e^{-\beta E_i(\gamma_l)}} \\ &= \left\langle \frac{\partial E_i(\gamma_l)}{\partial \gamma_l} \right\rangle \\ &\approx \frac{\partial \langle E_i(\gamma_l)\rangle}{\partial \gamma_l}, \end{aligned} \qquad \text{(B2)}$$

where γ_l denotes all the components of the γ-set defined in eq. (9). In addition, we have adopted an approximation assuming that the mean value of the derivative of the internal energy with respect to the components γ_l is approximately equivalent to the derivative of the mean value of this energy with respect to these components.[38]

Appendix C: Conductance calculation

The conductance is obtained from the Green's functions of the system. For the QD's $\alpha(\beta)$ we have the local Green's functions

$$G^\sigma_{\alpha\alpha(\beta\beta)} = \frac{\tilde{g}_{\alpha(\beta)\sigma}}{1 - t_{\alpha\beta}^2 \tilde{g}_{\alpha\sigma}\tilde{g}_{\beta\sigma}}, \qquad \text{(C1)}$$

obtained through a diagrammatic expansion which incorporates in the QD $\alpha(\beta)$ the physics underlying the complete system, including the electron reservoirs. The function $\tilde{g}_{\alpha(\beta)\sigma}$ that appears in this expression describes the sub-system composed by the QD $\alpha(\beta)$ connected to the $L(R)$ reservoir. The calculation of this function results in

$$\tilde{g}_{\alpha(\beta)\sigma} \;=\; \frac{g_{\alpha(\beta)\sigma}}{1 - t'^2 g_{\alpha(\beta)\sigma}\tilde{g}_{L(R)\sigma}}, \qquad \text{(C2)}$$

where $g_{\alpha(\beta)\sigma}$ is the single-particle Green's function associated with the QD $\alpha(\beta)$, while $\tilde{g}_{L(R)\sigma} = \frac{\omega - \sqrt{\omega^2 - 4t^2}}{2t^2}$ is the L(R) reservoir's Green's function projected onto its nearest QD $\alpha(\beta)$.

The non-local Green's functions of the system are given by

$$G^\sigma_{\alpha\beta(\beta\alpha)} \;=\; \frac{\tilde{g}_{\alpha(\beta)\sigma} t_{\alpha\beta} \tilde{g}_{\beta(\alpha)\sigma}}{1 - t_{\alpha\beta}^2 \tilde{g}_{\alpha(\beta)\sigma}\tilde{g}_{\beta(\alpha)\sigma}}, \qquad \text{(C3)}$$

and

$$G^\sigma_{L\alpha(R\beta)} \;=\; \frac{\tilde{g}_{L(R)\sigma} t' \tilde{g}_{\alpha(\beta)\sigma}}{1 - t_{\alpha\beta}^2 \tilde{g}_{\alpha\sigma}\tilde{g}_{\beta\sigma}} \qquad \text{(C4)}$$

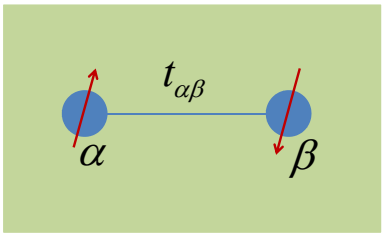

FIG. 11: (Color online) Schematic view of the decoupled DQD presented in Fig. 1.

which are associated to charge transport between the QDs and from the $L(R)$ reservoir to the QD $\alpha(\beta)$, respectively. This propagators can be used to obtain the conductance G of the system. Using $G^{\sigma}_{\alpha\beta}$, for example, we obtain from the Keldysh formalism[39] the following expression for the conductance:

$$G = \frac{2e^2}{h\pi^2} t_L^2 t_R^2 \int_{-\infty}^{+\infty} f_L(\omega) f_R(\omega) |G^{\sigma}_{\alpha\beta}(\omega)|^2 \frac{\partial f_{L(R)}}{\partial \omega} d\omega, \tag{C5}$$

where e is the electron charge, h is Planck's constant, and $f_{L(R)}(\omega)$ the Fermi distribution function associated to the L(R) reservoir.

Appendix D: Exact Solution of isolated DQD at half-filling

In order to better understand the characteristics of the antiferromagnetic and the Kondo molecular regime accessed when the DQD is at half- or quarter-filling, respectively, we calculate the exact solution when the DQD is decoupled from the metallic leads, as shown in Fig. (11). The exact solution obtained in this Appendix allows the identification of the regions in the parameter space corresponding to different regimes and the crossovers between them.

The Hamiltonian for the decoupled DQD in Fig. (11) is given by

$$H = \sum_{\substack{i=\alpha,\beta \\ \sigma}} \epsilon_i n_{i\sigma} + \sum_{i=\alpha,\beta} U_i n_{i\sigma} n_{i\bar{\sigma}} + \sum_{\sigma} t_{\alpha\beta} (c^{\dagger}_{\alpha\sigma} c_{\beta\sigma} + c^{\dagger}_{\beta\sigma} c_{\alpha\sigma}), \tag{D1}$$

where ϵ_i and U_i are respectively the energy of the local state and the Coulomb interaction in the i-th QD, $t_{\alpha\beta}$ is the hopping term and σ the spin projections of the electrons in the QDs. The DQD may have an electron occupancy of $N = 1, 2, 3, 4$. Thus, considering the system with two electrons, $N = 2$, we define the basis

$$|\varphi_1\rangle = |\uparrow\downarrow, 0\rangle \tag{D2}$$
$$|\varphi_2\rangle = |0, \uparrow\downarrow\rangle \tag{D3}$$
$$|\varphi_3\rangle = \frac{1}{\sqrt{2}}[|\uparrow,\downarrow\rangle - |\downarrow,\uparrow\rangle] \tag{D4}$$
$$|\varphi_4\rangle = \frac{1}{\sqrt{2}}[|\uparrow,\downarrow\rangle + |\downarrow,\uparrow\rangle] \tag{D5}$$
$$|\varphi_5\rangle = |\uparrow,\uparrow\rangle \tag{D6}$$
$$|\varphi_6\rangle = |\downarrow,\downarrow\rangle, \tag{D7}$$

where $|\varphi_1\rangle$, $|\varphi_2\rangle$ and $|\varphi_3\rangle$ are states with total spin $S_T = 0$, while $|\varphi_4\rangle$, $|\varphi_5\rangle$ and $|\varphi_6\rangle$ are states with $S_T = 1$. Written in this basis, the Hamiltonian can be separated into blocks, which correspond to the projections $S_T = 0$ and $S_T = 1$ of the total spin. The block-matrix that corresponds to a spin projection $S_T = 1$ is already diagonal and its eigenvalues are $E_4 = E_5 = E_6 = 2\epsilon_0$ (for simplicity we consider $\epsilon_\alpha = \epsilon_\beta = \epsilon_0$). These energies are associated to states with $S_T = 1$ and $S_z = 1, 0, -1$.

The block-matrix corresponding to $S_T = 0$ is given by

$$H^{AF}_{(2e)} = \begin{pmatrix} 2\epsilon_0 + U & 0 & -\sqrt{2}t_{\alpha\beta} \\ 0 & 2\epsilon_0 + U & \sqrt{2}t_{\alpha\beta} \\ -\sqrt{2}t_{\alpha\beta} & \sqrt{2}t_{\alpha\beta} & 2\epsilon_0 \end{pmatrix},$$

with the following eigenvalues:

$$E_1 = 2\epsilon_0 + U \tag{D8}$$
$$E_2 = \frac{1}{2}[4\epsilon_0 + U + \sqrt{U^2 + 16t^2_{\alpha\beta}}] \tag{D9}$$
$$E_3 = \frac{1}{2}[4\epsilon_0 + U - \sqrt{U^2 + 16t^2_{\alpha\beta}}]. \tag{D10}$$

These results allow (as shown in the Appendix A) a better understanding of the processes underlying the transition between the different regimes of the DQD.

* Corresponding author: martins@oakland.edu

[1] D. Goldhaber-Gordon, H. Shtrikman, D. Mahalu, D. Abusch-Magder, U. Meirav, and M. A. Kastner, Nature **391**, 156 (1998).
[2] W. Lu, Z. Ji, L. Pfeiffer, K. West, and A. Rimberg, Nature **423**, 422 (2003).
[3] Y. Ono, A. Fujiwara, K. Nishiguchi, H. Inokawa, and Y. Takahashi, Journ. Appl. Phys. **97** (2005).
[4] B. A. Jones, C. M. Varma, and J. W. Wilkins, Phys. Rev. Lett. **61**,

125 (1988).
[5] B. A. Jones and C. M. Varma, Phys. Rev. B **40**, 324 (1989).
[6] Note that the properties of this QCP are essentailly those of a two-channel Kondo (TCK) fixed point, see, for example, F.W. Jayatilaka, M. R. Galpin, and D. E. Logan, Phys. Rev. B 84, 115111 (2011).
[7] R. Bulla, T. A. Costi, and T. Pruschke, Rev. Mod. Phys. **80**, 395 (2008).
[8] O. Sakai and Y. Shimizu, J. Phys. Soc. Jpn. **68**, 2333 (1992).
[9] Further details on the properties of this critical point were obtained by Conformal Field Theory [I. Affleck and A. W. W. Ludwig, Phys. Rev. Lett. 68, 1046 (1992)] and Abelian bosonization [J. Gan, Phys. Rev. Lett. 74, 2583 (1995)].
[10] T. Aono, M. Eto, and K. Kawamura, J. Phys. Soc. Jpn. **67**, 1860 (1998).
[11] T. Aono and M. Eto, Phys. Rev. B **63**, 125327 (2001).
[12] R. Aguado and D. C. Langreth, Phys. Rev. Lett. **85**, 1946 (2000).
[13] E. Vernek, N. Sandler, S. E. Ulloa, and E. V. Anda, Physica E: Low-dimensional Systems and Nanostructures **34**, 608 (2006).
[14] B. Dong and X. L. Lei, Phys. Rev. B **65**, 241304 (2002).
[15] R. López, R. Aguado, and G. Platero, Phys. Rev. Lett. **89**, 136802 (2002).
[16] A. Georges and Y. Meir, Phys. Rev. Lett. **82**, 3508 (1999).
[17] P. Simon, R. López, and Y. Oreg, Phys. Rev. Lett. **94**, 086602 (2005).
[18] W. Izumida and O. Sakai, Phys. Rev. B **62**, 10260 (2000).
[19] C. A. Büsser, E. V. Anda, A. L. Lima, M. A. Davidovich, and G. Chiappe, Phys. Rev. B **62**, 9907 (2000).
[20] R. Aguado and D. C. Langreth, Phys. Rev. B **67**, 245307 (2003).
[21] R. H. Blick, D. Pfannkuche, R. J. Haug, K. v. Klitzing, and K. Eberl, Phys. Rev. Lett. **80**, 4032 (1998).
[22] T. H. Oosterkamp, T. Fujisawa, W. G. van der Wiel, K. Ishibashi, R. V. Hijman, S. Tarucha, and L. P. Kouwenhoven, Nature **395**, 873 (1998).
[23] H. Qin, A. W. Holleitner, K. Eberl, and R. H. Blick, Phys. Rev. B **64**, 241302 (2001).
[24] H. Jeong, A. M. Chang, and M. R. Melloch, Science **293**, 2221 (2001).
[25] E. Sela and I. Affleck, Phys. Rev. Lett. **102**, 047201 (2009), for more details, see J. Malecki, E. Sela, and I. Affleck, Phys. Rev. B **82**, 205327 (2010), where NRG calculations were performed.
[26] F. W. Jayatilaka, M. R. Galpin, and D. E. Logan, Phys. Rev. B **84**, 115111 (2011).
[27] J. Bork, Y.-h. Zhang, L. Diekhoner, L. Borda, P. Simon, J. Kroha, P. Wahl, and K. Kern, Nature Physics **7**, 047201 (2011).
[28] R. M. Potok, I. G. Rau, H. Shtrikman, Y. Oreg, and D. Goldhaber-Gordon, Nature **446**, 167 (2007).
[29] E. S. Sørensen and I. Affleck, Phys. Rev. B **53**, 9153 (1996).
[30] I. Affleck, L. Borda, and H. Saleur, Phys. Rev. B **77**, 180404 (2008).
[31] C. A. Büsser, G. B. Martins, L. Costa Ribeiro, E. Vernek, E. V. Anda, and E. Dagotto, Phys. Rev. B **81**, 045111 (2010).
[32] J. Simonin, ArXiv e-prints (2007), 0708.3604.
[33] G. Kotliar and A. E. Ruckenstein, Phys. Rev. Lett. **57**, 1362 (1986).
[34] The results in Fig. 2(B) should be compared to those in Fig. 2 of Ref. 18. Although the results presented there are for the even and odd 'molecular orbitals', the density of states suppression has the same origin.
[35] R. Žitko, J. Bonča, A. Ramšak, and T. Rejec, Phys. Rev. B **73**, 153307 (2006).
[36] E. V. Anda, G. Chiappe, C. A. Büsser, M. A. Davidovich, G. B. Martins, F. Heidrich-Meisner, and E. Dagotto, Phys. Rev. B **78**, 085308 (2008).
[37] E. Vernek, C. A. Büsser, G. B. Martins, E. V. Anda, N. Sandler, and S. E. Ulloa, Phys. Rev. B **80**, 035119 (2009).
[38] A. Cabrera and A. Calles, Rev. Mex. Fis. **36**, 385 (1989).
[39] L. V. Keldysh, Sov. Phys. JETP **20**, 1018 (1965).